Springer

KSME

Journal of Mechanical Science and Technology 24 (12) (2010) 2401~2411
www.springerlink.com/content/1738-494x
DOI 10.1007/s12206-010-0910-6

Identification of acoustic wave propagation in a duct line and its application to detection of impact source location based on signal processing †

Yong Woo Shin[1], Min Soo Kim[1] and Sang Kwon Lee[1*]

Department of Mechanical Engineering, Inha University, Seoul, 402-751, Korea

(Manuscript Received March 30, 2010; Revised July 29, 2010; Accepted August 9, 2010)

Abstract

For the detection of the impact location in a pipeline system, the correlation method has been the conventional method. For the application of the correlation method, the diameter of a duct should be small so that the acoustic wave inside the duct can propagate with non-dispersive characteristics, in the form of, for example, a plane wave. This correlation method calculates the cross-correlation between acoustic waves measured at two acceleration sensors attached to a buried duct. It also gives information about the arrival time delay of an acoustic wave between two sensors. These arrival time delays are used for the estimation of the impact location. However, when the diameter of the duct is large, the acoustic waves inside the duct propagate with dispersive characteristics owing to the reflection of the acoustic wave off of the wall of the duct. This dispersive characteristic is related to the acoustic modes inside a duct. Therefore, the correlation method does not work correctly for the detection of the impact location. This paper proposes new methods of accurately measuring the arrival time delay between two sensors attached to duct line system. This method is based on the time-frequency analyses of the short time Fourier transform (STFT) and continuous wavelet transform (CWT). These methods can discriminate direct waves (non-dispersive waves) and reflective waves (dispersive waves) from the measured wave signals through the time-frequency analysis. The direct wave or the reflective wave is used to estimate the arrival time delay. This delay is used for the identification of the impact location. This systematic method can predict the impact location due to the impact forces of construction equipment with more accuracy than the correlation method.

Keywords: Impact signal; Duct acoustic; Arrival time delay; Wavelet transform; Correlation method; Dispersive wave; Direct wave

1. Introduction

In a buried gas duct, the impact force by a construction machine is often a cause of duct damage and gas leakage. Gas leakage induces many serious problems, such as explosions, energy loss and environmental pollution. Therefore, early detection of an impact location is an important task. When an impact force excites a buried duct, an elastic wave is generated on the surface of the duct that excites the gas inside the duct. The elastic wave is attenuated by the damping of the soil around a buried duct [1], but the excited gas generates an acoustic wave that propagates in the downstream direction, as shown in Fig. 1.

There have been many theoretical and experimental studies of gas leakage problems in pipeline systems [1-3]. In these investigations, in order to detect a gas leak in a pipeline system, the correlation method [4] was typically used as a conventional method. This method uses the arrival time delay of the acoustic waves propagating inside a pipe. The arrival time delay of acoustic waves is measured by two sensors attached to the surface of the pipeline. In this case, the acoustic wave of the gas inside a pipeline is regarded as a plane wave which propagates only in the axial direction because the propagation of a wave in the radial direction can be neglected when the diameter of the pipe is small. Therefore, measuring the arrival time delay of an acoustic wave between two sensors is straightforward because the phase speed of an acoustic wave with the characteristics of a plane wave is constant and is not dependent on the frequency. The impact location is predicted using the measured arrival time delay and the known distance between two sensors. However, in the case of a duct with a large diameter, the acoustic wave propagates not only in the axial direction but also in the radial direction. The wave that propagates in the axial direction does not reflect, but the wave in the radial direction reflects off of the wall of the duct. The former is a direct wave with non-dispersive characteristics. The latter is a reflective wave with dispersive characteristics. The direct wave has a constant phase speed. The phase speed

† This paper was recommended for publication in revised form by Associate Editor Yeon June Kang

*Corresponding author. Tel.: +82 32 860 7305, Fax.: +82 32 868 1716
E-mail address: sangkwon@inha.ac.kr

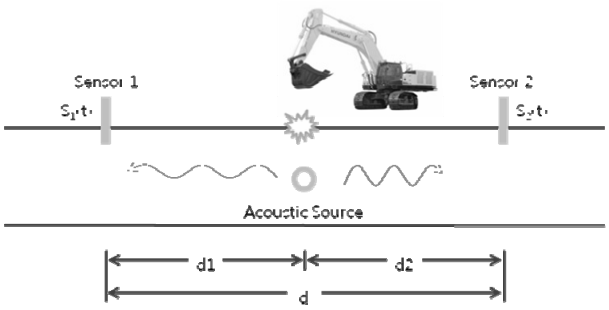

Fig. 1. Propagation process of the acoustic wave generated by the impact excitation of construction machinery.

of the reflective wave is dependent on the frequency. This dispersive wave propagation is related to the acoustic cavity modes and cut off frequencies which are determined by the geometry of the duct. For a duct line system with a large diameter, a correlation method based on the plane wave cannot predict the impact location in a duct system. The present study proposes new methods to predict the impact location in a duct line gas supply system. The proposed methods are based on the time-frequency method which estimates the arrival time delay of an acoustic wave between two sensors attached to the duct line. This time delay can be used for the prediction of the impact location with a high level of accuracy. The time-frequency method can identify the dispersive characteristics of an acoustic wave in the time-frequency domain and discriminate between the reflective wave with its dispersive property and the direct wave with its non-dispersive property.

In this paper, STFT and CWT are considered using the time frequency method. STFT does not have good time resolution but has good frequency resolution depending on the signal. CWT has good time resolution, although it has a wide frequency resolution at a high frequency. Therefore, STFT was initially used to discriminate between a direct wave and a reflective wave, as the frequency resolution is important in this discrimination. As a subsequent step, CWT was used to estimate the arrival time delay of the direct wave, and STFT was used to estimate the arrival time delay of the reflective direct wave. These two different methods are carefully applied to a laboratory test for validation and successfully applied to an actual duct line system with greater accuracy than the correlation method. In particular, if the pipe is embedded partially within a very wet soil or it is partially or fully exposed to the water, the wave propagation within the pipe system containing some amount of dense gases or fluid will be very different than that was stated in this paper. In section 2, the dispersive phenomenon in duct acoustics is assessed by acoustic theory and in experiments. In section 3, new methods are developed for the prediction of the impact location. In section 4, the correlation method is briefly explained for a comparison with the proposed method. In section 5, this method is applied to an actual duct system. In the last section, the results are discussed with conclusions.

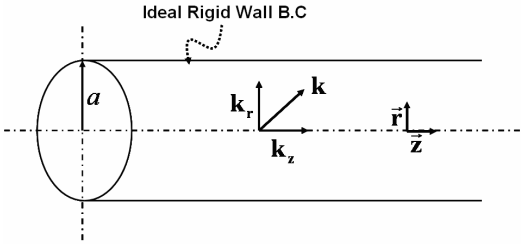

Fig. 2. Boundary condition and cylindrical axis for an acoustic wave analysis of a duct.

2. Acoustic wave in a duct

2.1 Theory of wave propagation in a circular duct

The linear, three-dimensional, lossless, homogeneous wave equation in the cylindrical coordinate system [5-7] is given by

$$\nabla^2\phi(t,\mathbf{r})-\frac{1}{c^2}\frac{\partial^2}{\partial t^2}\phi(t,\mathbf{r})=0\,, \tag{1}$$

where $\phi(t,\mathbf{r})$ is the velocity potential at time t and position $\mathbf{r}=(r,\theta,z)$ and c is the speed of sound. If a duct has a circular cross-section, the inside wall of the duct is ideal rigid and the length of the duct is infinite in the z-direction, the velocity potential of the time-harmonic eigenfunctions is

$$\phi(t,r)=\sum_{m,n=0} A_{mn}J_m(k_{rmn}r)\cos(m\theta)e^{jk_{zmn}z}e^{-j\omega t}, m,n=0,1,2.. \tag{2}$$

In Eq. (2), k_{zmn} is the axial wave number and k_{rmn} is the radial wave number.

They can be specified by ordered integers (m,n). For the cylindrical waveguide with the coordination shown in Fig. 2, the wave number k is related to the axial number k_{zmn} and the radial wave number k_{rmn} through the following equation:

$$k_{zmn}=\sqrt{k^2-k_{rmn}^2}\,, m,n=0,1,2,... \tag{3}$$

As the normal component of velocity vector must be equal to zero on the rigid boundary at $r=a$, from Eq. (2),

$$J'_m(k_{rmn}a)=\frac{\partial}{\partial r}[J_m(k_{rmn}r)]_{r=a}=0, m,n=0,1,2... \tag{4}$$

Here, for a given value of integer m, n, there are infinitely many values of $k_{zmn}a$ that will satisfy Eq. (4). Thus, the radial wave number is given by

$$k_{rmn}=\frac{j'_{mn}}{a},\ m,n=0,1,2...\,, \tag{5}$$

and the cut off frequency f_{rmn} is given by

$$f_{rmn}=\frac{cj'_{mn}}{2\pi a},\ m,n=0,1,2,... \tag{6}$$

where j'_{mn} is the extremum of the first kind of Bessel functions. Substituting Eq. (5) and Eq. (6) into Eq. (3), the axial wave number becomes

$$k_{zmn} = k\sqrt{1-\left(\frac{f_{rmn}}{f}\right)^2}\ , \quad f \geq f_{rmn}\ . \tag{7}$$

From Eq. (2), the normal acoustic modes associated with cut off frequencies f_{rmn} are given by

$$\phi_{mn} = J_m(k_{rmn}r)\cos(m\theta)\ , \quad (0 < r < a)\ . \tag{8}$$

In Eq. (8), the integer m determines the number of radial nodal lines, and the second integer n determines the number of azimuthally nodal lines. In Eq. (7), if the driving frequency f is high enough, $f > f_{rmn}$ and $k_{zmn} > 0$, the acoustic wave with the (m, n) mode shape propagates downstream along the waveguide of the duct. All modes with cut-off frequencies below the driving frequency f can propagate energy and can be seen at large distances. At the cut-off frequency, $f = f_{rmn}$ and $k_{zmn} = 0$, there is no longitudinal acoustic wave motion. If the driving frequency f is low enough, $f < f_{rmn}$ and $k_{zmn} < 0$, k_{zmn} must be pure imaginary, the acoustic wave with the (m, n) mode shape does not propagate and its amplitude decays exponentially. The axial wave number k_{zmn} given in Eq. (3) is used for the expression of the acoustical propagation without considering the flow of the fluid in a duct. However, when the fluid flows with constant velocity V along the duct, it should be modified. The modified axial wave number is given by [8],

$$k_{zmn} = \frac{-Mk \pm \sqrt{k^2 - k_{rmn}^2(1-M^2)}}{1-M^2}, \tag{9}$$

where M is the Mach number expressed as $M = V/c$. The modified cut-off frequency is $f'_{rmn} = f_{rmn}\sqrt{1-M^2}$ and the modified axial wave number is $k'_{rmn} = k_{rmn}\sqrt{1-M^2}$. The only difference from the cut-off frequency f_{rmn} is the effect of the Mach number. However, if the flow speed V is small, the Mach number is small and the effect of the flow can therefore be neglected. The phase speed of an acoustic mode is observed in Eq. (3) to be

$$c_p = \frac{\omega}{k_{rmn}} = \frac{c}{\sqrt{1-(f_{rmn}/f)^2}}, \tag{10}$$

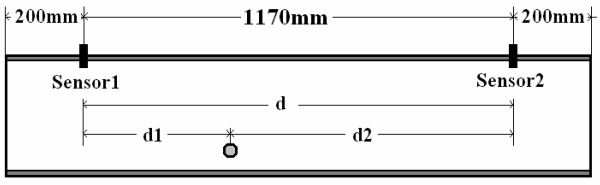

Fig. 3. Geometry of the cylinder duct used in this research and location of the acoustic source and two microphones.

and is clearly not equal to c. The phase speed is dependent on the cut-off frequency f_{rmn}. Therefore, the acoustic wave inside the duct propagates downstream with continual reflection off of the walls. Thus, the group speed c_g at which speed energy moves in the z direction is given by the component of the plane wave velocity c along the waveguide axis z:

$$c_g = c\sqrt{1-(f_{rmn}/f)^2}\ . \tag{11}$$

This reflective effect of the wall becomes the cause of the dispersive phenomenon of the acoustic wave propagation inside the duct.

2.2 Experimental validation for theory of wave propagation

When an impact force excites a circular duct, as shown in Fig. 3, the impact location can be identified using the arrival time delay between two sensors attached to the circular duct. The arrival time delay is obtained by dividing the distance between the two sensors by the group speed of the acoustic wave inside the duct. If the acoustic wave inside the duct is a plane wave, the phase speed and the group speed of the acoustic wave are equal to the sound speed of the gas inside the circular duct. If the diameter of the duct is small enough, the acoustic wave inside the duct is regarded as a plane wave. However, if the diameter is large enough, the acoustic modes of the duct influence the wave propagation inside the duct waveguide.

Two types of wave propagations exist inside a duct. The first is the propagation of a direct wave, and the second is the propagation of a reflective wave. The phase speed of the direct wave is constant and equal to the speed of sound for the gas inside a circular duct. The direct wave is not affected by the reflection of the acoustic wave off of the wall. The direct wave is also not dependent on the cut-off frequency and thus the non-dispersive wave. Its acoustic mode is related to the (0,0) mode among an infinite number of (m, n) modes. On the other hand, the phase speed of the reflective wave is affected by the reflection of the acoustic wave off of the wall. This speed is obtained through Eq. (10). The reflective wave is dependent on the cut-off frequency and thus becomes a dispersive wave. The phase speed of the reflective wave is affected by the acoustic mode on the order of (m, n). Therefore, the group speed of the reflective wave as well is not constant and dependent on the cut-off frequency. It is obtained through Eq. (11). In this section, the cut-off frequencies f_{rmn}, acoustic modes, the phase speed c_p and the group speed c_g are calculated by the theoretical method discussed in the previous section. They are also estimated by a measurement method based on the time-frequency method. The results obtained by both methods are compared to validate the theoretical results. Through this experimental validation, the dispersive phenomenon of the acoustic wave in a circular duct was identified, and the reflective and direct waves were discriminated. Fig. 3 shows the geometric dimensions of the duct used in this test.

Table 1. Theoretical cut-off frequencies f_{rmn} (Hz) of a steel pipe (diameter =106 mm, sound speed for the laboratory air =343.4m/s).

n / m	0	1	2	3	4
0	0.00	3878.3	7108.6	10298.3	13488.1
1	1863.2	5397.2	8647.7	11857.7	15047.5
2	3088.4	6794.6	10095.8	13336.2	16556.3
3	4253.0	8121.2	11493.2	14774.1	18014.5
4	5387.1	9397.1	12840.0	16161.4	19442.3

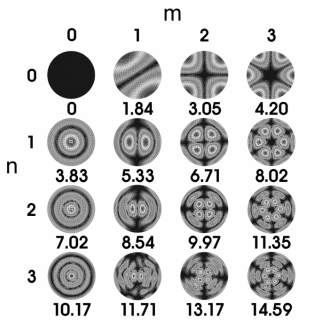

Fig. 4. Mode shapes and frequencies associated with the (m, n) mode for the acoustic cavity of the cylinder duct used in this research.

The inside diameter of the duct is 106mm, the thickness is 4mm and the length is 1570mm. The cut-off frequencies f_{rmn} of the test duct were theoretically calculated using Eq. (6). These are listed in Table 1. The acoustic mode shapes of the circular duct related to the cut-off frequency f_{rmn} were obtained using Eq. (8), as illustrated in Fig. 4. Using Eq. (10) and Eq. (11), the phase speed c_p and the group speed c_g were also theoretically calculated. The Mach number is not considered in this validation test. The sound speed of air used in this calculation is 340m/s. The group and phase speeds were calculated theoretically.

These are plotted in Fig. 5. These results show that the sound speed of the direct wave related to the (0,0) mode, which is propagated down without a reflection process on the wall of the waveguide, is 340 m/s. The curves above and below the (0,0) mode respectively show the phase speed and the group speed of the reflective waves related to the (m, n) order mode. To validate the analytically calculated cut-off frequencies listed in Table 1 and the two types of speeds, experimental work proceeds with a circular duct waveguide, as shown in Fig. 3.

The duct was installed in the full anechoic chamber shown in Fig. 6, and two microphones were inserted into the duct to measure the sound pressure inside it. A sound with a frequency-modulated signal was generated by a specially designed loudspeaker in the middle of the duct. The frequency of the modulated signal was increased from 100Hz to 5 kHz during a very short time. Two microphones were located at d_1 = 540mm and d_2 = 630mm from the loudspeaker, respectively.

The sound pressures measured using these two microphones were analyzed by signal processing technology. The traditional method for measuring the cut-off frequencies related to acoustic modes in a duct is to use the power spectrum density (PSD) [9]. This result is shown in Fig. 7. The power spectral density function S_{xx} (f) for sound press signal x is defined by

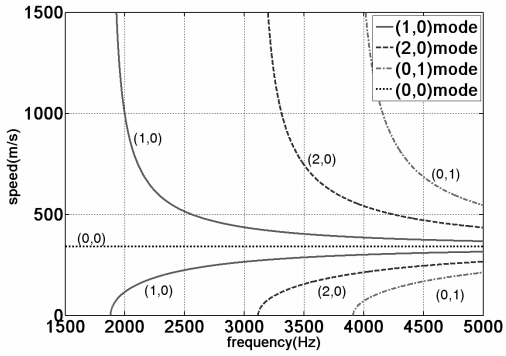

Fig. 5. Behavior of the group and phase speeds as function of the frequency for the three cavity modes in the duct waveguide used in this research.

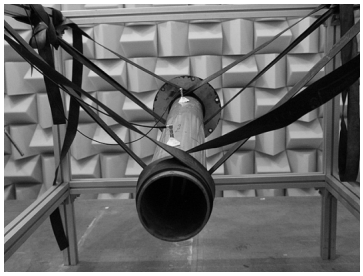

Fig. 6. Photograph of the test duct installed in the full anechoic chamber for the investigation of the acoustic propagation characteristics.

$$S_{xx}(f) = \lim_{T\to\infty} \frac{E\left[\left|X_T(f)\right|^2\right]}{T}, \tag{12}$$

where X_T (f) is the Fourier transform of signal x and T is the averaging time. According to a PSD analysis of signal x, the PSD cannot show the dispersive phenomenon of the wave, although the information pertaining to the three cut-off frequencies is roughly presented.

To observe the dispersive phenomenon, a time-frequency analysis was applied to sound press signal x. The time frequency method used in this test was STFT. The STFT for sound press signal x is defined by [10],

$$S_x(f,t) = \int_{-\infty}^{\infty} x(\tau) h^*(\tau - t) e^{-j2\pi f\tau} d\tau\,, \tag{13}$$

where h (t) is a short window function. Fig. 8 shows the STFT results of the data measured by the two microphones.

The process for the identification of the acoustic modes in a duct is explained through the analysis of an image plot, as shown in Fig. 8. In this figure, the horizontal axis represents the time and the vertical axis is the frequency. The solid lines of the center part in each map correspond to the peak amplitude, which refers to the distribution of the acoustic energy

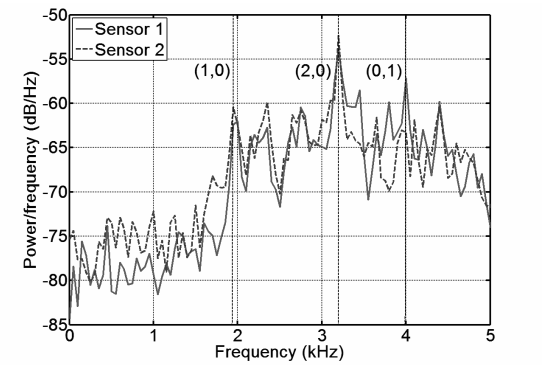

Fig. 7. Power spectrum density analysis for the sound pressure signals measured using two microphones: (a) Sensor 1 at position d_1, (b) Sensor 2 at position d_2.

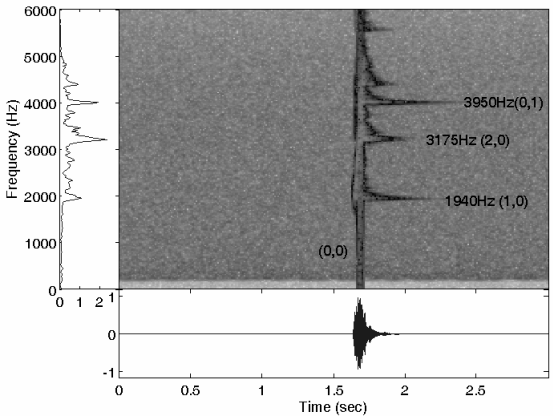

(a)

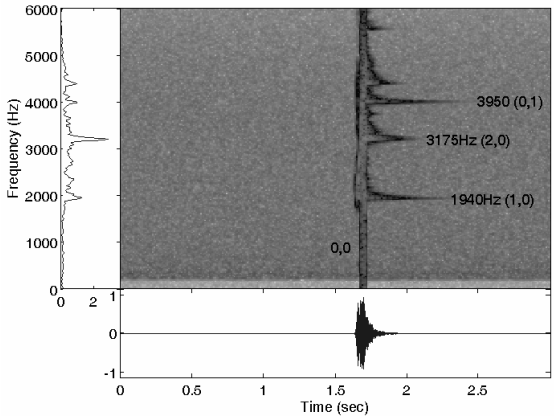

(b)

Fig. 8. Short time Fourier transform for the measured sound pressure signals using two microphones: (a) Sensor 1 at position d_1, (b) Sensor 2 at position d_2.

due to the propagation of the wave. The cut-off frequencies for mode (1,0), mode (2,0) and mode (0,1) were determined to be 1940Hz, 3175Hz and 3950 Hz, respectively. There are slight differences among these results (calculated results are listed in Table 1). These differences average approximately

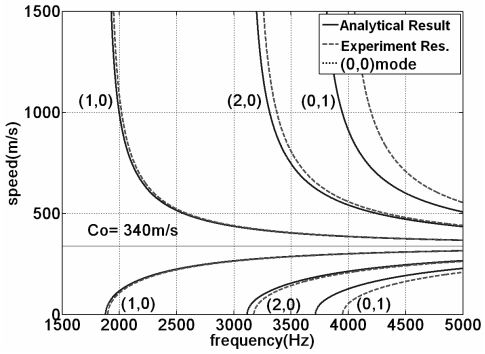

Fig. 9. Comparison between the calculated wave speeds and the measured wave speeds.

3.8% due to the use of the time-frequency resolution of the STFT method [11]. However, the dispersive phenomenon can be determined through the STFT results. In Figs. 8(a) and (b), the time difference between the starting point of the signal and the solid line representing the dispersive curves is the arrival time of the waves generated by the impact source inside the duct from the impact location to each sensor. By dividing the distance from the impact point to the sensor by this time difference, the group velocity associated with each (m, n) mode can be estimated. These results are plotted in a comparison with the theoretical results, as shown in Fig. 9.

From these results, the dispersive phenomenon due to the reflection off of the rigid wall was identified at each acoustic mode. The trends of the experimental results correspond very well to the theoretical results. Some of the difference between the theoretical results and the measured results at high-order modes is caused by the time resolution problem in the STFT method, as mentioned earlier. With this approach, there is some difficulty in estimating the phase speed of the direct wave because the time resolution of the vertical line that represents the arrival time of the direct wave associated with the (0,0) mode is too wide, as shown in Figs. 8(a) and (b). Therefore, a time frequency method with good time resolution is necessary for the estimation of the phase speed of the direct wave associated with the (0,0) mode. To overcome the aforementioned problems, the CWT is utilized. These results are presented in the next section.

3. Identification of impact location based on time-frequency method

In the previous section, an acoustical theory for wave propagation in a duct was investigated and validated through novel experimental work. The dispersive characteristic, cut-off frequencies and the speeds of the wave were experimentally identified. In this section, two methods are developed to predict the impact location. The first method involves the use of a non-dispersive direct wave based on the wavelet transform, and the second method involves the use of a dispersive wave based on the STFT method. These two prediction methods are compared with the correlation method.

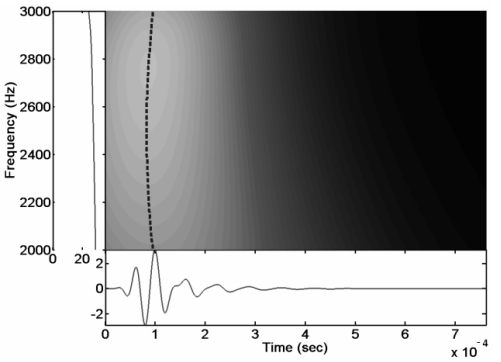

(a)

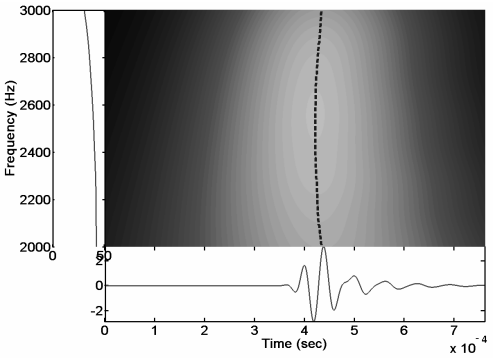

(b)

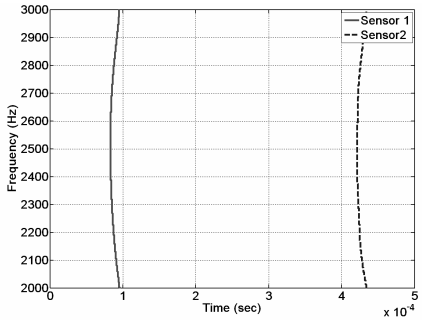

(c)

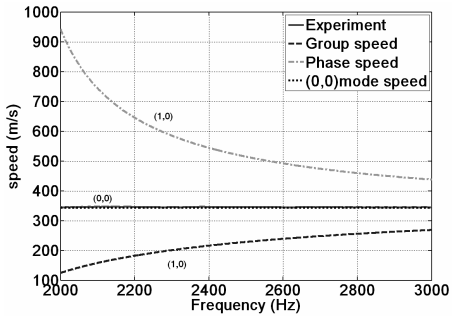

(d)

Fig. 10. Estimation of the arrival time delay between two sensors using a direct wave based on wavelet transforms: (a) wavelet transform for the direct wave measured by sensor 1, (b) wavelet transform for the direct wave measured by sensor 2, (c) the wave front of the direct wave, (d) the estimated sound speed of the direct wave and the reflective wave with the (1,0) mode.

3.1 Prediction of Impact Location based on CWT of the direct wave

In the prediction of the impact location in a buried duct using two sensors, the speed of wave c and arrival time delay τ between two sensors are required. The distances d_1 and d_2 from the impact location to both sensors can then be identified using the equation below:

$$d_{1,2} = \frac{d \mp c\tau}{2}, \qquad (d_1 < d_2)\ . \tag{14}$$

Here, d is the distance between the two sensors and the known value. The speed of wave c is generally the sound speed of a plane wave. When reflective waves are used, as in Eq. (14), the sound of speed c is replaced by the group speed c_g of the reflective waves associated with the (m, n) mode. In a duct, the direct wave is non-dispersive and its sound speed is identical to the speed of sound of the (0, 0) mode. To measure the arrival time delay of the direct wave at two sensors, the peak line representing the arrival time of the wave associated with the (0,0) mode in the time-frequency domain must be narrow. However, with the STFT method, the peak lines related to the (0,0) mode have a wide band resolution, as shown in the Figs. 8(a) and (b). This wide time resolution cannot predict the arrival time precisely. In this section, the CWT with good time resolution is employed. The CWT is based upon a family of functions [12],

$$\psi_{a,b}(t) = \frac{1}{\sqrt{a}}\psi\left(\frac{t-b}{a}\right), \quad a > b \in \Re\,, \tag{15}$$

where ψ is a fixed function, known as the "mother wavelet," that is localized both in time and frequency. The function $\psi_{a,b}(t)$ is obtained by applying the operations of shifting (b-translation) in the time domain and scaling in the frequency domain (a-dilation) to the mother wavelet. The mother wavelet used throughout this paper is the Morlet wavelet [12],

$$\psi\ (t) = \frac{1}{\sqrt{\pi B}} e^{j\omega_0 t - (t^2/B)}\,, \tag{16}$$

where ω_0 is the center frequency of the mother wavelet and B is the bandwidth defined as the variances of the Fourier transform $\Psi(f)$ of the Morlet wavelet:

$$B = \int_{-\infty}^{+\infty} f^2 \Psi^*(f) df \quad . \tag{17}$$

The CWT of a signal $x(t)$ is defined by

$$W_x^{\psi}(a,b) = \int_{-\infty}^{+\infty} x(t)\psi_{a,b}^*(t)dt = \frac{1}{\sqrt{a}}\int_{-\infty}^{+\infty} x(t)\psi^*\left(\frac{t-b}{a}\right)dt, \tag{18}$$

where $\psi^*(\cdot)$ is the complex conjugate of $\psi(\cdot)$. Additionally, the function $x(t)$ satisfies the following condition:

$$\|x\|^2 = \int_{-\infty}^{+\infty} |x(t)|^2 \, dt < +\infty \, . \tag{19}$$

Here, $\psi_{a,b}(t)$ plays a role analogous to $e^{j\omega t}$ in the definition of the Fourier transform.

If the mother wavelet, $\psi(t)$, satisfies the admissibility condition, then

$$C_\psi = \int_{-\infty}^{+\infty} \frac{|\Psi(\omega)|^2}{|\omega|} d\omega < +\infty \quad . \tag{20}$$

The inverse wavelet transform can be obtained by solving the following equation:

$$x(t) = \frac{1}{C_\psi} \int_{-\infty}^{+\infty} \int_{-\infty}^{+\infty} W_x^\psi(a,b) \psi_{a,b}(t) \frac{dbda}{a^2} \, , \tag{21}$$

An alternative formulation of the CWT, Eq. (18), can be obtained by expressing $x(t)$ and $\psi(t)$ via their Fourier transforms X (ω) and Ψ (ω), respectively:

$$W_x^\psi(a,b) = \sqrt{a} \int_{-\infty}^{+\infty} X(\omega) \Psi^*(a\omega) e^{j\omega b} d\omega \quad . \tag{22}$$

The relationship between the scale parameter a and frequency ω can be expressed as [13, 14]:

$$a = \frac{\omega_0}{\omega} \, , \tag{23}$$

where is the center frequency of the mother wavelet (see (15)). In terms of signal processing, a wavelet basis generates a constant-Q octave-band or octave band filter bank structure [15, 16]. Therefore, the frequency resolution is good at low frequencies and the time resolution is good at all frequencies. Therefore, the wavelet transform is a better solution for a time-frequency analysis of impact signals with a high frequency component [17-19]. For the wavelet analysis of the signal measured through the two microphones, the Morlet wavelet was used for the mother wavelet.

To obtain a direct wave that does not contain the effect of a dispersive wave, a band pass filter (BPF) was applied to the measured signal before the wavelet transform. The frequency band of the BPF was selected using the STFT results, as shown in Fig. 8. To obtain a pure direct wave, the frequency component between an arbitrary (m, n) mode should be used as the frequency bandwidth of the BPF. In this paper, a filtered wave containing a frequency component between the (1,0), and (2,0) modes was selected as the direct wave. The selected frequency band was therefore located between 2000 Hz and 3000Hz. The wavelet transform was applied to the filtered wave. Figs. 10(a) and (b) show the results of the wavelet transform for filtered waves of two signals measured by sensor 1 and sensor 2, respectively. The contour map and image analysis of the waves in the time-frequency space are shown in the center part. In the figures, the horizontal axis represents the time and the vertical axis represents the frequency. The dashed lines in the center part in each map correspond to the peak amplitude; these are plotted together in Fig. 10(c). The time difference shown in Fig. 10(c) becomes the arrival time delay τ between the two sensors. The time delay is about 350microsecond. The sound speed corresponding to this arrival time delay was calculated and the results plotted, as shown in Fig. 10(d). According to these results, the phase speed of the direct waves associated with the (0,0) mode is approximately 343± 2m/s. The group speed and phase speed of the (1,0) mode calculated theoretically using Eq. (11) are also plotted together with the speed of the direct wave. As the phase speed of the direct waves is identical to the sound speed of air in an anechoic chamber, it is 343m/s at 20°C. These results allow the conclusion that the arrival time delay τ of an acoustic wave due to an acoustic source can be estimated precisely using the CWT instead of the STFT. With this measured arrival time delay τ and the sound speed c of the fluid in the duct, the locations d_1 and d_2 are determined using Eq. (14). Fig. 11 shows the location of the acoustic source loudspeaker from sensor 1 and sensor 2. According to these results, the estimation of the acoustic source by the time-frequency method is effective considering that the distance errors are 0.6%. The average error is 1mm and the maximum error is 4.2mm for distance d_1 and distance d_2.

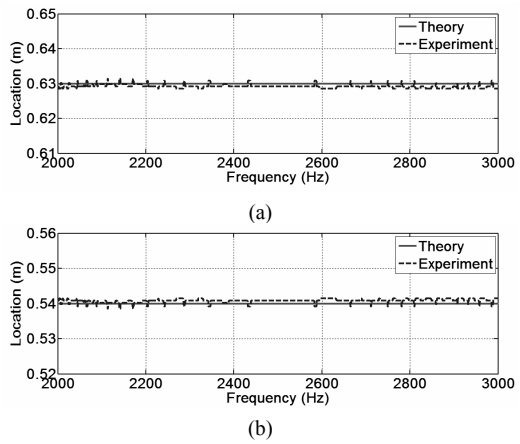

Fig. 11. Detection of the acoustic source location via time-frequency based on the CWT method: (a) distance d_1 of sensor 1, (b) distance d_2 of sensor 2.

3.2 Prediction of the Impact Location based on the STFT of the reflective wave

There are many reflective waves with the (m, n) mode, as shown in Figs. 8(a) and (b). Among these modes, the reflective wave of the (1, 0) mode has been used to estimate the arrival time delay τ.

In Figs. 8(a) and (b), the horizontal axis represents the time and the vertical axis represents the frequency. The curved lines corresponding to the peak amplitude of the (1,0) mode

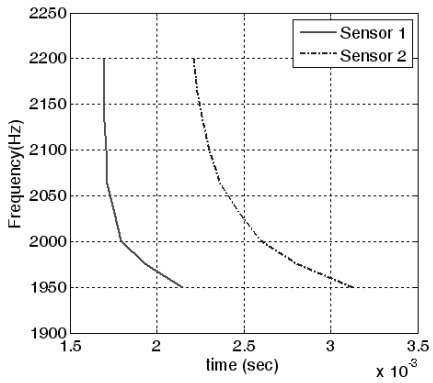

Fig. 12. Estimation of the arrival time delay between two sensors.

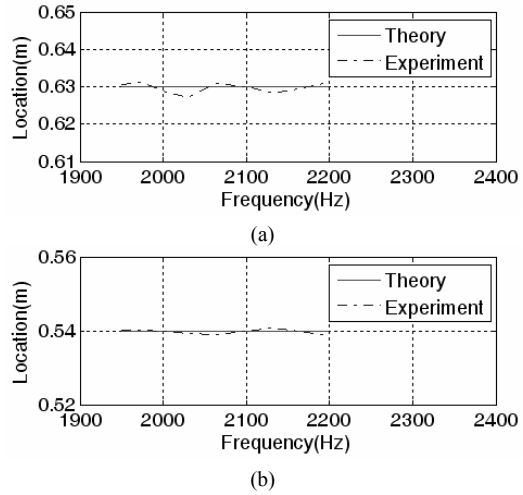

Fig. 13. Detection of the acoustic source location via a time-analysis of the reflective wave: (a) distance d_1 of sensor 1, (b) distance d_2 of sensor 2.

are plotted in the same time-frequency domain, as shown in Fig. 12.

The time difference between both lines becomes the arrival time delay τ between the two sensors. The time delay τ depends on the frequency, as the group speed depends on the frequency. The group speed and phase speed of the (1,0) mode were calculated theoretically using Eq. (11). These results are plotted in Fig. 9. The group speeds of the (1,0) mode and the time delay τ are used for the prediction of distances d_1 and d_2 from the impact location. Fig. 13 shows a comparison of the predicted distance and the true distance. According to these results, the impact locations predicted by the CWT method mode correspond very well to the true impact locations. The prediction error of the impact location is less than 1%.

4. Correlation method

As with the conventional method, the cross-correlation for the raw signals measured from the two sensors was used for the detection of the source location. In this study, a cross-correlation of the filtered signals was investigated and compared with the time-frequency method for the detection of the impact location. The frequency band of the filter was selected using the PSD method for raw signals. From Fig. 7, the frequency band containing the three major modes is determined. The frequency band between 1,900 Hz and 5,000Hz was selected for the filtering of the raw data [1, 4]. The cross-correlation function is given by

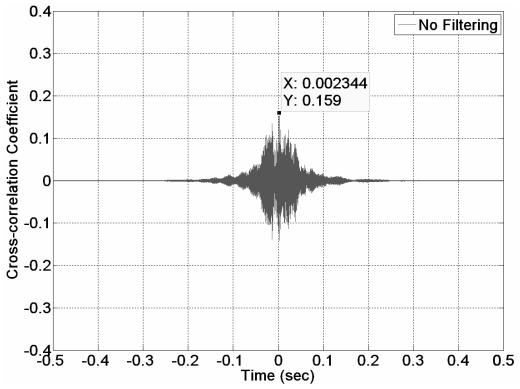

Fig. 14. Cross-correlation of the data measured by sensor 1 and sensor 2.

$$R_{s_1 s_2}(\tau) = E[s_1(t), s_2(t+\tau)]. \tag{24}$$

Here, $s_1(t)$ and $s_2(t)$ are the acoustic signals of sensor 1 and sensor 2, respectively, and τ is the time delay. To normalize the value of Eq. (24), the maximum auto-correlation data was used. Eq. (24) is the normalized cross-correlation function.

$$\rho_{s_1 s_2}(\tau) = \frac{R_{s_1 s_2}(\tau)}{\sqrt{R_{s_1 s_1}(0), R_{s_2 s_2}(0)}}. \tag{25}$$

In this equation, $R_{s_1 s_1}(0)$ and $R_{s_2 s_2}(0)$ are the auto-correlation maximum values. The distance d1 is calculated using Eq. (14). In this test, two distances, d1 and d2, were used to estimate the source location.

Fig. 14 shows the cross-correlation at a distance of 630mm. According to these results, the estimation distance d_1 obtained through the use of a filtering signal is 180mm. The error for each data instance is close to 66%. This error is too great to ignore for the detection of the impact location in a long industrial duct. Therefore, the correlation method is not a viable means of detecting the impact location in a duct with a large diameter.

5. Application

A practical experiment was carried out using a buried duct. Fig. 15 shows an image of the impact process in the duct. Two acceleration sensors instead of microphones were respectively installed at distances of 7km and 13km from the impact location.

Surface vibration of the buried duct was generated by the excitation of an acoustic wave at the sensor attachment point.

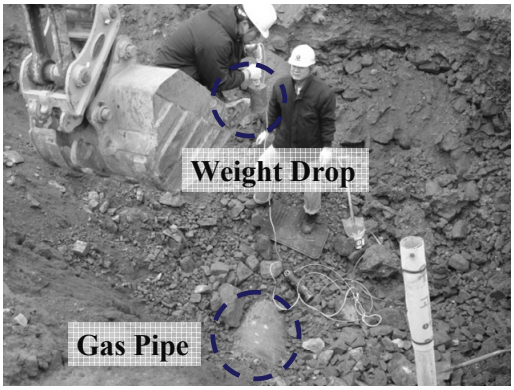

Fig. 15. Photograph of the impact process used to measure the wave propagation properties of a buried gas duct.

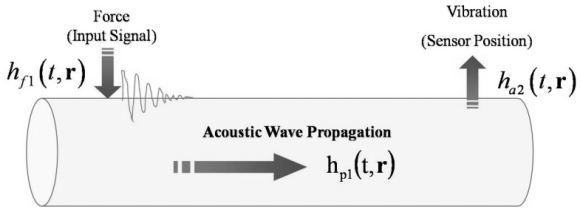

Fig. 16. Propagation process of the acoustic wave generated by the excitation of an impact force in a long buried duct.

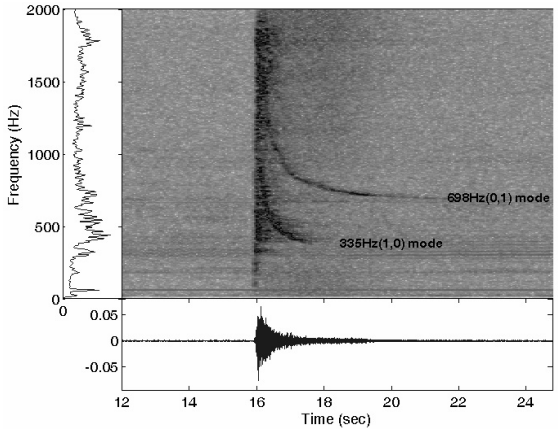

Fig. 17. Short time Fourier transform of the acceleration signals measured using two accelerometers located 7km from impaction position shown in Fig. 15.

This acoustic wave was generated by the excitation of the impact force. It propagated to the sensor attachment point. Therefore, the vibration signal indirectly provides information pertaining to the impact force. This type of propagation process for an acoustic wave is illustrated in Fig. 16.

The propagation of an elastic wave on the surface of the test duct is damped by the soil around the duct and then decays along the duct line. This type of wave propagation was simulated by a numerical method [20, 21]. In this simulation, three impulse responses $h(t,r)$ were used. Therefore, in this paper, to detect the impact location, only the acoustic wave inside the duct was considered, as this wave propagates over a long distance. The vibration signal measured on the surface of the duct

Table 2. Theoretical cut-off frequencies *frmn* (Hz) of a steel pipe (diameter=762 mm, sound speed for the gas=436 m/s).

m \ n	0	1	2	3	4
0	0	698	1279	1853	2427
1	335	971	1556	2134	2708
2	556	1223	1817	2400	2979
3	765	1461	2068	2659	3242
4	969	1691	2311	2908	3499

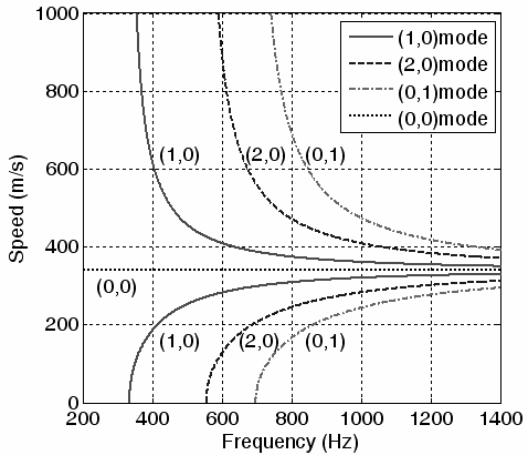

Fig. 18. Behavior of the group and phase speeds as a function of the frequency for three cavity modes in the duct waveguide used as an actual gas duct in this study.

at a long distance can represent the propagation characteristics of the acoustic wave because the elastic wave is decayed by soil damping.

Fig. 17 shows the results of the time-frequency analysis of the measured acceleration signal using the STFT method. Although there is a filtering effect due to the thickness of the duct, the dispersive characteristic of the acoustic wave can be observed clearly, as shown in Fig. 17.

The dispersive phenomenon of the acoustic wave results from the reflection at the rigid wall; it is dependent on each acoustic mode. The flow speed of the gas is 4m/s. The sound speed of the gas is 438 ± 2 m/s [22]. As the Mach number M is approximately 0.009132, the cut-off frequency f_{rmn} does not change very much. Therefore, the effect of the Mach number was ignored. The sound speed c of gas in a buried duct is 438m/s. The diameter of the duct in this case was 78cm. The calculated cut-off frequency of the buried duct is listed in Table 2.

The cut-off frequency can be also estimated using the STFT results of an acceleration signal measured at sensor 1, as shown in Fig. 17. The STFT results for the acceleration signal measured at sensor 2 were obtained using a similar pattern. The dominant cut-off frequencies obtained by applying the STFT to the measured data were 335 Hz and 698Hz and correspond to the cut-off frequency of the (1,0) mode and (0,1) mode, respectively. The dispersive waves associated with

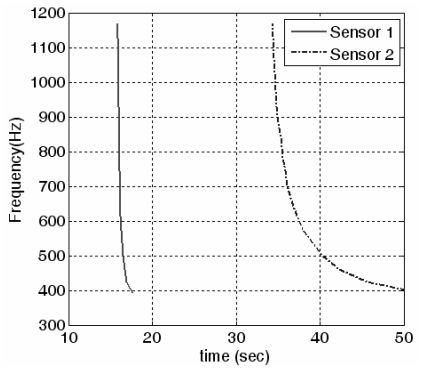

Fig. 19. Estimation of the arrival time delay between two sensors using the time difference of the peak amplitudes caused by the energy transmission of an acoustic wave in the time-frequency domain.

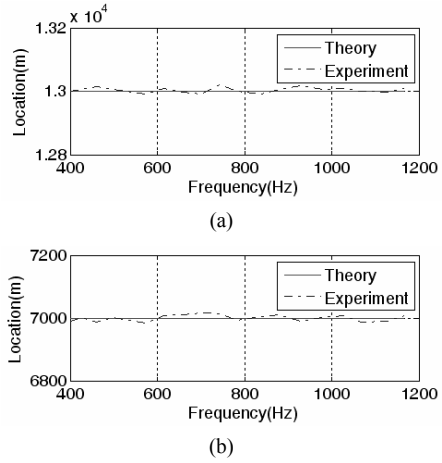

Fig. 20. Detection of the acoustic source location via a time-analysis of the reflective wave in an actual duct: (a) distance d_1 of sensor 1, (b) distance d_2 of sensor 2.

these two acoustic cavity modes carry the acoustic energy to the sensor locations. The direct wave also carries the acoustic energy without reflection; it is propagated with a wide frequency component as the wave front includes the energy over the entire frequency region. It arrives at the sensor attachment point sooner than the dispersive waves.

This direct wave can be used to estimate the arrival time delay of an acoustic wave. However, as shown in Fig.17, the use of the direct wave for the prediction of the impact location is problematic because determining the non-dispersive region remains a challenge. Therefore, the reflective wave with the (1,0) mode is used for the estimation of the impact location. For an actual gas duct, the group speed and phase speed of the (1,0) mode and other three modes calculated theoretically using Eq. (11) were also plotted, as shown in Fig. 18.

The peak amplitude line corresponding to the dispersive curve of the (1,0) mode in time-frequency analysis was selected and plotted together with the peak amplitude line obtained using the data measured at sensor 2, as shown in Fig. 19. The time difference becomes the arrival time delay τ between two sensors. The time delay τ depends on the frequency, as the group speed depends on the frequency. The group speed of the (1,0) mode and the time delay τ were used for the prediction of the distances d_1 and d_2 from the impact location. Fig. 20 shows the location of the acoustic source loudspeaker from sensor 1 and sensor 2, respectively. According to these results, the estimated value of the acoustic source using the reflective wave of the (1,0) mode correspond very well to the true locations. The estimated error is less than 1 %.

6. Discussion and conclusions

The cut-off frequencies in a duct were calculated based on the theory of wave propagation. These cut-off frequencies were also estimated using a novel experimental method. The results were shown to be in good agreement with the theoretical results. The dispersive characteristic around the cut-off frequencies was clearly identified via CWT and STFT time-frequency analyses. Through the time-frequency analysis, the direct wave with a non-dispersive characteristic and the reflective wave with a dispersive characteristic were identified. To predict the impact location in a duct with a large diameter, the group speeds of both waves were estimated theoretically. The arrival time delay between two sensors was measured using two proposed methods. The first of these involves the use of the direct wave based on the CWT, and the second method involves the use of the reflective wave based on the STFT method. The theoretically estimated group speed and arrival time delay were used for the prediction of the impact location in a duct line system. The impact location predicted using the CWT method or the STFT method was compared with that obtained from a conventional correlation method. The prediction error of the impact location obtained using the two methods proposed in this study was determined to be less than 1%. However, the conventional method used with pipeline systems with a small diameter yields a prediction error of 60%.

Acknowledgment

This work was supported by the National Research Foundation of Korea (NRF) grant funded by the Korea government (MEST) (No. 2009-0084728) and (No. 2010-0014260).

References

[1] J. M. Muggleton and M. J. Brennan, Leak Noise Propagation and Attenuation in Submerged Plastic Water pipes, *Journal of Sound and Vibration*, 278 (3) (2006) 527-537.

[2] H. V. Fuchs and R. Riehle, Ten Years of Experience with Leak Detection by Acoustic Signal Analysis, *Applied Acoustics,* 33 (1) (19991) 1-19.

[3] W. T. Chu, Acoustical Characteristics of Leak Signals in Plastic Water Distribution Pipes, *Applied Acoustics*, 58 (3) (1997) 235-254.

[4] S. B. M. Beck, M. D. Curren, N. D. Sims and R. Stanway, Pipeline Network Features and Leak Detection by Cross-Correlation Analysis of Reflected Waves. *Journal of Hy-*

draulic Engineering, 131 (8) (2005) 715-723.

[5] M. L. Munjal, *Acoustics of Ducts and Mufflers with Application to Exhaust and Ventilation System Design*, Wiley, New York , USA (1987).

[6] L. E. Kinsler, et al. *Fundamentals of Acoustics*, Wiley, New York, USA (1999).

[7] J. G. Ih and B. H Lee, Analysis of higher-order mode effects in the circular expansion chamber with mean flow, *J. Acoust. Soc. Am.*, 77 (1985) 1377-1388.

[8] V. Mason, Some Experiments on the Propagation of Sound along a Cylindrical Duct Containing Flowing Air. *Journal of Sound and Vibration*, 10 (2) (1969) 208-226.

[9] K. Shin and J. K. Hammond, *Fundamentals of Signal Processing for Sound and Vibration Engineers*, Wiley, London, UK, 2008.

[10] S. K. Lee and R. White, Fault Diagnosis of Rotating Machinery Using Wigner Higher Order Moment Spectra, *Mechanical Systems Signal Processing*, 11 (4) (1997) 637-650.

[11] S. K. Lee, S. Banerjee and A. Mal, Identification of Impact Force on a Thick Plate Based on the Elastodynamics and Higher-Order Time-Frequency Analysis, *Proceedings of the Institution of Mechanical Engineers Part C, Journal of Mechanical Engineering Science*, 221 (11) (2007) 1249-1263.

[12] S. K. Lee, An Acoustic Decay Measurement Based on Time-Frequency Analysis Using Wavelet Transform, *Journal of Sound and Vibration*, 252 (1) (2002) 141-152.

[13] Teolis, Computational Signal Processing with Wavelets. Birkhäuser, Boston, USA (1999).

[14] S. Mallat, A Wavelet Tour of Signal Processing, *Academic Press*, New York (1999).

[15] R. M. Rao and A. S. Bopardikar, Wavelet Transforms Introduction to Theory and Applications, Prentice Hall, New York (1999).

[16] T. ÖnsAy and A. G. Haddow, Wavelet Transform Analysis of Transient Wave Propagation in a Dispersive Medium, *The Journal of the Acoustic Society of America*, 95 (3) (1999) 1441-1449.

[17] D. E. Newland, An Introduction to Random Vibrations, Spectral & Wavelet Analysis, Longman Scientific & Technical Press, London, UK (1994).

[18] S. K. Lee and P. R. White, The Enhancement of Impulsive Noise and Vibration Signals for Fault Detection in Rotating and Reciprocating Machinery, *Journal of Sound and Vibration*, 217 (3) (1998) 485-505.

[19] S. K. Lee and P. R. White, Application of Wavelet Analysis to the Impact Harshness of a Vehicle, *Proc. Institute of Mechanical Engineers, Journal on Mechanical Engineering* Science, Part C, 214 (11) (2002) 1331-1338.

[20] M. S. Kim, S. K. Lee, Y. J. Jang and J. P. Koh, Acoustic Wave Propagation Characteristics Corresponding to the Cut-off Frequency in Gas Pipeline, *Journal of The Korean Society for Noise and Vibration Engineering*, 18 (7) (2008) 693-700.

[21] S. J. Kim, S. G. Kim, K. S. Oh and S. K. Lee, Excitation Force Analysis of a Powertrain based on CAE Technology, *International Journal of Automotive Technology*, 9 (6) (2008) 703-711.

[22] L. Burstein, D. Ingman and Y. Michlin, Correlation between Gas Molecular Weight, Heating Value and Sonic Speed under Variable Compositions of Natural Gas, *ISA Transactions*, 38 (4) (1999) 347-359.

Sang-Kwon Lee obtained his B.S. in Mechanical Engineering at Pusan National University. In 1998 he received the Ph.D. in Signal Processing at the ISVR (Institute of Sound and Vibration Research) of the University of Southampton in U.K. He has 11 years' experience in automotive noise control at Hyundai Motor Co. and the Renault-Samsung Motor Company in Korea. In 1999, he moved to Inha University, Inchon, Korea, where he became a professor and continued research on the acoustics and vibration signal processing in the Department of Mechanical Engineering.

Yong Woo Shin is a graduate student in the Department of Mechanical Engineering at Inha University. He has studied the application of signal processing to acoustics and vibration in a duct.